

---

## High Frequency Structure-borne Sound Simulations using a hybrid Dynamical Energy Analysis / Advanced Transfer Path Analysis Approach

Gregor TANNER<sup>1</sup>; Satoshi MORITA<sup>2</sup>; Timo Hartmann<sup>1</sup>; Martin RICHTER<sup>1</sup>

<sup>1</sup> University of Nottingham, United Kingdom

<sup>2</sup> Yanmar R&D Europe s.r.l, Italy

### ABSTRACT

Dynamical Energy Analysis (DEA) is a mesh-based high frequency method modelling structure borne sound for complex built-up structures. This has proven to enhance vibro-acoustic simulations considerably by making it possible to work directly on existing finite element meshes circumventing time-consuming and costly remodeling strategies. In addition, DEA provides detailed spatial information about the vibrational energy distribution within a complex structure in the mid-to-high frequency range. DEA was successfully applied and validated to a structure borne sound calculation of an assembled agricultural tractor. Modelling solid structures is still a challenge for DEA, however, as it is based on 2D wave transmission calculations. We propose a novel method to generate DEA elements based on measurement data in order to model solid parts of a complex structure. Advanced Transfer Path Analysis (ATPA) is employed to extract energy transmission characteristics of a structure. First, Frequency Response Functions are measured between interface points on a structure. Then a direct transfer function between interface points is calculated by using ATPA. Finally, DEA elements connecting interface points and representing energy transmission characteristics of the structure are created based on the ATPA result. Applications of the method will be presented.

Keywords: High frequency structure borne sound, DEA, ATPA

### 1. INTRODUCTION

Simulations of the vibro-acoustic performance of cars, trains, airplanes as well as heavy goods vehicles such as lorries and tractors are routinely carried out at various design stages. To understand the transmission of structure-borne sound in such mechanical structures, it is necessary to have effective and efficient modelling tools to support the structural design process, ideally before a prototype vehicle is built. Numerical calculations are widely used to aid the understanding and estimation of noise and vibrations. In particular, the Finite Element Method (FEM) is used routinely for noise and vibration simulations in complex structures in the low frequency regime. It requires extremely fine meshes at high frequencies, however, to capture shorter wave lengths leading to large model sizes. Additionally, since the structural response at high frequencies is very sensitive to small variations in material properties and boundary conditions, the simulation result from FEM become less reliable. Statistical representations such as the Statistical Energy Analysis (SEA) [1] have been developed, leading to relatively small and simple models in comparison with FEM. SEA has found widespread applications in the automotive and aviation industry, as well as in architectural acoustics. However, SEA is based on a set of often hard to verify assumptions, which effectively require diffuse wave fields and quasi-equilibrium of wave energy within sub-systems. In addition, SEA gives results only on a relatively coarse scale and cannot deal with details of the structure [2,3,4].

Here, we start from a ray-tracing ansatz reformulated in terms of integral equations. This leads to linear flow equations for the mean vibrational energy density and forms the basis of the Dynamical Energy Analysis

---

<sup>1</sup> gregor.tanner@nottingham.ac.uk

(DEA) method introduced first in [5]. DEA includes SEA as special case via a low order representation of the so-called transfer operator. Higher order implementations enrich the DEA model with information from the underlying ray dynamics, leading to a relaxation of SEA assumptions. In particular, DEA allows for more freedom in sub-structuring the total system and variations of the energy density across sub-structures can be modelled. Hence, DEA can resolve the full geometrical complexity of the structure. An efficient implementation of DEA on meshes has been presented in [6, 7]. Vibro-acoustic energy densities are computed for multi-modal propagation, including energy transport over curved surfaces. Connections at material interfaces are described in terms of reflection/transmission matrices. DEA has been used to calculate the structure borne sound of an assembled agricultural tractor and good agreement between measurements and DEA calculations have been shown [8]. In particular, it has been demonstrated that DEA can model shell structures accurately. However, it is still difficult to model a solid structure because currently DEA is based on wave transmission calculations through plate/plate junctions. Additionally, it is often difficult to generate accurate FE meshes of assembled complex structures because of welds, bolts and rubber bushes between each of the components. To overcome these limitations, we suggest to integrate measurement data into DEA to improve the effectiveness of DEA modelling.

In this paper, we propose a novel method to generate DEA elements based on the Advanced Transfer Path Analysis (ATPA) [11]. ATPA is employed to extract energy transmission characteristics of a structure. Firstly, Frequency Response Functions (FRFs) are measured between interface points on a structure. Then the direct transfer functions between all interface points are calculated using ATPA. Finally, DEA elements connecting interface points and representing energy transmission characteristics of the structure are created based on the ATPA result. The proposed method is verified with a finite element model of a simple structure.

## 2. Theory

### 2.1 Dynamical Energy Analysis on meshes

We will give a brief account of the major ideas behind DEA here – for a detailed description of the theory and the implementation on 2D meshes, see [6, 8]. In the high frequency regime, the dynamics described by linear wave equations can be approximated using semi-classical or ray-tracing methods describing the transition from wave acoustics to ray acoustics; this serves as a starting point for DEA. By neglecting phase information, DEA approximates the transport of wave energy by a Hamiltonian flow [5] described by the *Liouville equation*. The flow is phase space volume preserving and can be formulated in terms of trajectories or *rays*. In contrast to ray tracing, DEA does not work with individual rays, but describes how ray densities are transported along the flow. In this work we are primarily interested in the stationary solution of transport problems corresponding to wave problems in the frequency domain with time-harmonic driving terms. Interference (or phase) effects are neglected.

The ray density can be related to a wave energy density and is defined on a phase space, that is, it depends both on position and direction. For two-dimensional systems (as considered in this work), the phase space is four dimensional and is parametrized by two position and two momentum coordinates. The momentum coordinates are equivalent to the wave vector. For fixed frequency  $\omega$  and a given wave mode, the modulus of the wave vector, that is, the wavenumber, is fixed. Hence, there is only one free parameter necessary to describe the direction.

The transport problem can be conveniently solved on a mesh as described in [6, 8]. In particular, it is advantageous to restrict the Hamiltonian flow to sections on the union of all the edges of the mesh describing the two-dimensional structure in question. The coordinates used to describe this restricted two-dimensional phase space, the so-called Surface of Section (SoS), are the arc-length along each edge  $i$ ,  $s_i$ , and the corresponding component of the wave vector along the direction of the edge,  $p_i$ . The continuous Hamiltonian flow is thus transformed into a discrete map, also called the Discrete Flow Map (DFM) [6].

DEA describes the transport of ray densities from the SoS to itself using a linear transfer operator which is now discretised and represented as a matrix with entries of the form [6, 8]

$$T_{(i,l',m')|(j,l,m)} = \frac{2m+1}{2\sqrt{A_{l'}A_l}} \int_0^{A_l} \int_{-c_j^{-1}}^{c_j^{-1}} w_{rt}(p'_i) e^{-\nu L(s_j,s'_i)} P_{m'}(p'_i) P_m(p_j) dp_j ds_j,$$

where  $P_m$  is a scaled Legendre polynomial of order  $m$  as detailed in [8], and the energy is propagated along a trajectory through the mesh element  $j$  with propagation speed  $c_j$ . This trajectory starts at position  $s_j$  on edge  $l$  of element  $j$  and is transported to position  $s'_i$  on the common edge  $l'$  of the boundary of element  $i$ . The tangential component of the momentum (or slowness) of the trajectory at  $s_j$  is denoted  $p_j$  and likewise for  $p'_i$  at  $s'_i$ . Note, that  $p'_i$  and  $s'_i$  are uniquely determined by  $p_j$  at  $s_j$ . Also  $L(s_j,s'_i)$  is the length of the trajectory from  $s_j$  to  $s'_i$ ,  $\eta$  is a (viscous) damping parameter. Furthermore,  $A_l$  is the length of edge  $l$  from element  $j$ , and likewise  $A_{l'}$  is the length of edge  $l'$  from element  $i$ . The weight function  $w_{rt}$  gives the reflection/transmission coefficients which are obtained from wave scattering theory [9]. Mode conversion between in-plane and flexural waves at boundaries can be included in the treatment. Shell effects leading to curved rays [10] are included by treating the meshed structure as set of plate-like elements, see [6-8] for details.

Once the matrix  $B$  has been constructed, the energy density on the boundary phase-space of each element is given by the solution of a linear system of the form

$$(\mathbf{I} - \mathbf{T})\rho_0 = \rho$$

where  $\mathbf{I}$  is the identity matrix and  $T$  has entries as defined by equation (1). Here,  $\rho_0$  is the initial density produced by a source term. Once  $\rho$  has been computed, the energy density at any location inside the structure can be computed in a post-processing step.

## 2.2 DEA-TPA modelling

In many practical applications, providing meshes for some parts of the structure may be very time-consuming and thus costly due the internal complexity of the parts. Typical examples are the engine, the gear-box or the drive train as a whole and adjacent parts. In these circumstances, it would be easier to do local measurements and include effective transmission parameters into the DEA calculation. In order to extract the energy transmission parameters, the Transfer Path Analysis (TPA) approach is taken here [11]. The DEA-TPA method is based on the same principle as the RBE-patch method introduced in [8]. The difference to the RBE-patch method is that we use frequency dependent transition rates obtained from measurements. Energy transitions are assumed to take place between connecting interfaces. Labelling the interfaces with  $k, k' = 1, n$ , we define a transition matrix  $S_{k,k'}$  between these interfaces. An interface is normally made up of different edges of the mesh. Let us assume the edge  $E_{b''}$  is part of interface  $k$  and the edge  $E_{b'}$  is part of interface  $k'$  which is shown in Figure 1. We now allow a transition between  $E_b$  and  $E_{b'}$  via the edge  $E_{b''}$  using the equation,

$$\tilde{T}_{(b',\beta')|(b,\beta)} = \left[ \sum_{\tilde{k}} S_{\tilde{k},k} \right] \frac{S_{k',k} A_{b'}}{\sum_{\tilde{k}} S_{\tilde{k},k} \sum_{\tilde{b} \in J_{\tilde{k}}} A_{\tilde{b}}} T_{(b',\beta')|(b,\beta)} \quad (1)$$

Here,  $A_b, A_{b'}$  are the lengths of the edges  $E_b, E_{b'}$ ,  $\beta, \beta'$ , the indices for the momentum basis and  $T_{(b',\beta')|(b,\beta)}$  is the transfer operator matrix element between two edges not including weighting factors. The first term in (1) represents overall damping, the fraction in the middle gives the relative transition rates for a single edge. The denominator represents the total outgoing energy flux from interface  $k$ .

In [8], the RBE-patch method was introduced to account for coupling between different sub-meshes provided by an FE-modeler. For combining measurement results with DEA, we determine the rates for the transition matrix  $S$  using the ATPA method which is ideal to derive local transition rates from global response functions. The basic theory of ATPA is described in the next session.

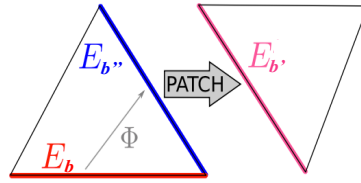


Figure 1: Schematic sketch of the connection between mesh edges using patch elements

### 2.3 Advanced Transfer Path Analysis

ATPA is a variant of the transmission path analysis method using so-called Direct Transfer Functions (DTFs) calculated from a Global Transfer Functions (GTFs) [11]. The GTFs correspond to the common concept of a measurable transfer function. The GTFs represent transitions between measured points via all transmission path. The DTF elements represent the quotient between two specific points where all the other paths remain blocked.

The GTF  $G_{ij}^g$  from point  $i$  to  $j$  is defined as the scenario where one applies an external excitation  $f^{ext}$  (for example a force) at point  $i$  and the external excitation at all other points is set to zero [11], that is,

$$G_{ij}^g = \frac{S_j}{S_i} \text{ with } f^{ext}(0, \dots, 0, f_i^{ext}, 0, \dots, 0)^T \quad (2)$$

where  $s_i$  and  $s_j$  represent a measured signal which can describe quantities such as acceleration, velocity, displacement or energy. The DTF  $T_{ij}^D$  from  $i$  to  $j$  is defined as the scenario where one applies an external excitation at point  $i$  with vanishing external excitation at point  $j$  and vanishing displacements at any point other than  $i$  or  $j$ , that is

$$G_{ij}^D = \frac{S_j}{S_i} \text{ with } S_k = 0, k \neq i, j. \quad (3)$$

As already mentioned, the DTF between two points gives the quotient of their signals when all the other points in the system are blocked. Consequently, the DTF is normally difficult to measured but it can be calculated by using the GTF as follows:

$$G_{kk}^D = \frac{1}{[(G^g)^{-1}]_{kk}} \quad (4)$$

$$G_{jk}^D = \frac{-[(G^g)^{-1}]_{jk}}{[(G^g)^{-1}]_{kk}} \text{ for } j \neq k. \quad (5)$$

In this paper, an energetic approach of the ATPA is employed as we focus here on the mid-high frequency regime. In the energetic approach, the measured signal  $s_i$  represents the energy at point  $i$ . Therefore, the energy density is used which is calculated using

$$s_i = \rho h v_i^2 \quad (6)$$

where  $\rho$  is the material density,  $h$  is the thickness of the plate and  $v_i$  is the velocity at point  $i$ .

### 3. FE model for DEA-TPA

In order to validate the DEA-TPA approach, the method is tested with an FE model of a simple structure made up of three plates connected via 4 connecting beams. We assume that the middle plate, plate 2,

represents the complicated part and is modelled as the DEA-TPA element. Four interface points are defined at the boundaries of the connecting beams as shown in Figure 2. The GTFs is calculated here using FEM instead of measuring a real structure, validation is also performed doing an FE calculation of the full structure. To define the transition matrix described in Eq. (1), several steps are introduced as follows:

- We first normalise the outgoing flow to 1, that is

$$\tilde{G}_{ij}^D = G_{ij}^D / \sum_j G_{ij}^D$$

- We then  $S_{ji} = \tilde{G}_{ij}^D$  set in the case that interface  $i$  and  $j$  are not on the same plate.
- The diagonal terms correspond to reflection from the interface and we set  $S_{ii} = \tilde{G}_{ii}^D + \tilde{G}_{ij}^D$  if  $i$  and  $j$  are on the same plate.
- We set  $S_{ij} = 0$ , if  $i$  and  $j$  are different points on the same plate.

The excitation point is on plate 1 (lower right plate) and shown in Figure 2.

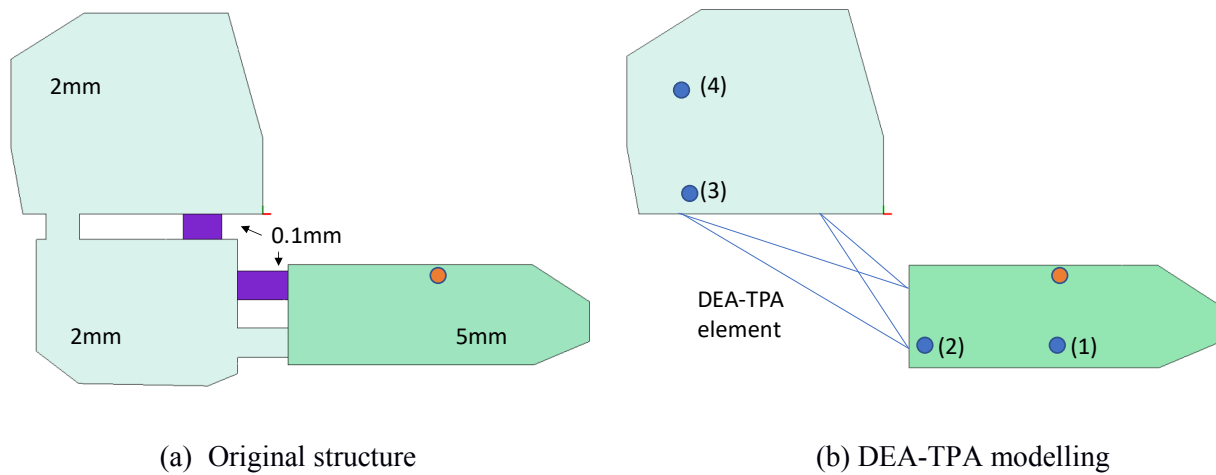


Figure 2: The FE models for the full structure and the TPA model. The thicknesses of the plates are shown in the left figure. The orange dot shows excitation point. The blue dots give measurement points, see the results in Figure 4.

## 4. Results

### 4.1 Energy distribution

Entities of the transition matrix are calculated based on Eq. (4) and (5). However, for frequencies below 1000Hz negative value of the calculated GTFs have been observed. Therefore, here, we focus on the frequency above 1000Hz for the ATPA results. Figure 3 shows a comparison of the acceleration distributions between averaged FEM result over 1/3 frequency band, a full DEA calculation and DEA-TPA result for 2500 Hz. Figure 4 also shows results for the energy calculated at the points depicted in Figure 2 clearly demonstrating that both the DEA and the DEA-TPA capture the energy distributions accurately at 2500 Hz. A comparison between DEA, DEA-TPA results and FEM at selected points and over the full frequency range from 250Hz to 2500Hz are presented in Figure 5 showing good agreement over the whole frequency range.

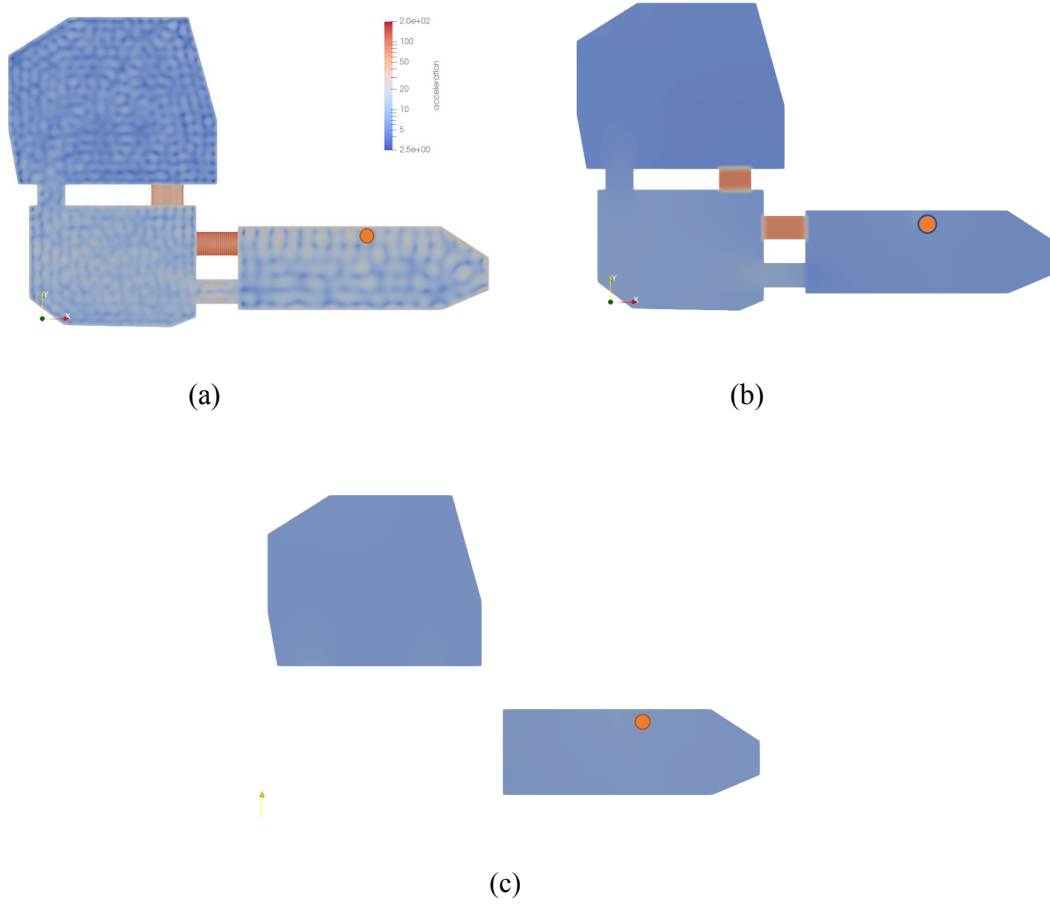


Figure 3: Comparison of FEM, DEA and DEA-TPA model at 2500Hz; (a) averaged FEM over 1/3 octave frequency region at 2500Hz, (b) DEA and (c) DEA – TPA

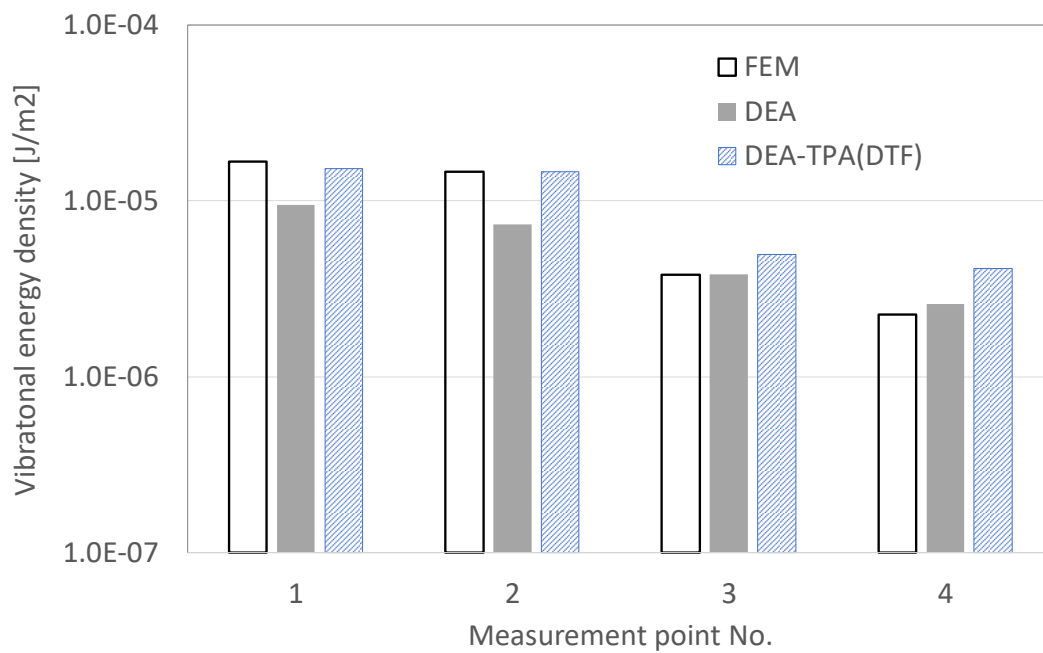


Figure 4: Comparison of FEM, DEA and DEA-TPA model at 2500Hz

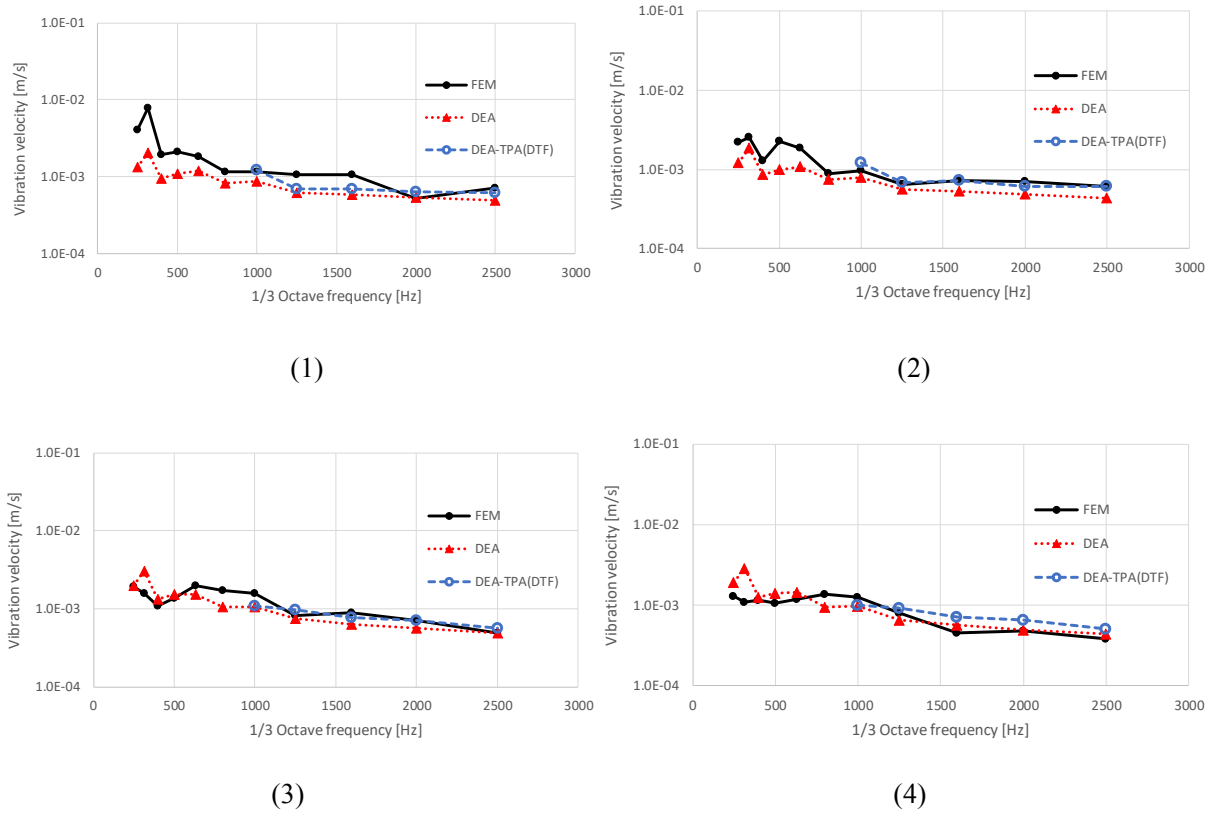


Figure 5: Comparison of FEM, DEA and DEA-TPA model over the frequency range 250Hz to 2500Hz.

## 4.2 Energy flow calculations

The ray density  $\rho(\mathbf{r}, \mathbf{p})$  computed in DEA provides more information than just the energy density. In particular, it allows one to estimate the momentum density vector  $\mathbf{I}(\mathbf{r})$  (sometimes called intensity vector) directly, and thus gives information about the direction of mean energy flow at each point on the structure. This can be done as a post-processing step by computing the vectoral quantity

$$\mathbf{I}(\mathbf{r}) \propto \int \mathbf{p} \varrho(\mathbf{r}, \mathbf{p}) d\mathbf{p}$$

at each point on the structure. Here  $\mathbf{r}$  is the position and  $\mathbf{p}$  is the (two-dimensional) momentum variable.

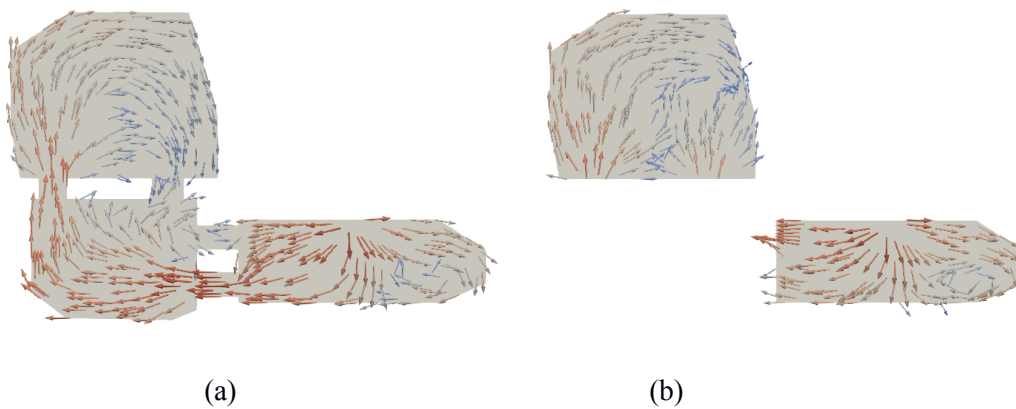


Figure 8: Comparison of calculated energy flow between DEA and DEA-TPA at 1600Hz

## 5. Conclusions

In this paper, the DEA-TPA modelling method was proposed and compared with an FEM calculation. It was shown how ATPA input can be integrated into a transition matrix calculation giving rise to a hybrid DEA-TPA method. Both the DEA-TPA modelling as well as a DEA computation compares favorably with the FEM results with DEA-TPA giving a slightly more accurate description as expected.

## References

1. R. H. Lyon, and R. G. DeJong, Theory and Application of Statistical Energy Analysis, Butterworth-Heinemann, Boston, 1995.
2. P. J. Shorter and R. S. Langley, Vibro-acoustic analysis of complex systems, *Journal Sound Vib.*, Vol. 288, 669-699, 2005.
3. V. Cotoni, P.J. Shorter, and R.S. Langley, Numerical and validation of a hybrid finite element-statistical energy analysis method, *J. Acoust. Soc. Am.*, 122, 259-270, 2007.
4. G. Xie, L. Dunne, A. Secgin and A. Zoghaib, Mid-frequency modelling of a car floor structure with hybrid method and SEA, *International Symposium on the Computational Modelling and Analysis of Vehicle Body Noise and Vibration*, 2012, Sussex, UK.
5. G. Tanner, Dynamical energy analysis - Determining wave energy distributions in vibro-acoustical structures in the high-frequency regime, *J. Sound Vib.* 320, 1023-1038, 2009.
6. D. J. Chappell, G. Tanner, D. Lochel and N. Sondergaard, Discrete flow mapping: transport of phase space densities on triangulated surfaces, *Proc. R. Soc. A*, 469, 20130153, 2013.
7. D. J. Chappell, D. Lochel, N. Sondergaard and G. Tanner, Dynamical energy analysis on mesh grids: A new tool for describing the vibro-acoustic response of complex mechanical structures, *Wave Motion* 51, 589-597, 2014.
8. T. Hartmann, S. Morita, G. Tanner, and D. J. Chappell, High-frequency structure-borne sound transmission for a tractor model using Dynamical Energy Analysis, *Wave Motion* 87, 132-150, 2019.
9. R. S. Langley and K. H. Heron, Elastic wave transmission through plate/beam junctions, *J. Sound Vib.* 143, 241, 1990.
10. A. N. Norris and D. A. Rebinsky, Membrane and Flexural Waves on Thin Shells, *ASME J. Vib. Acoust.* 116, 457-467, 1994.
11. O. Guasch, F. X. Magrans, The Global Transfer Direct Transfer method applied to a finite simply supported elastic beam, *J. Sound Vib.*, 276, 335-359, 2004